J. Nannoplankton Res. **37** (2–3), 2017, pp.177–188 © 2017 International Nannoplankton Association
ISSN 1210-8049 Printed by The Sheridan Press, USA

Biostratigraphic and morphometric analyses of specimens from the calcareous nannofossil genus *Tribrachiatus*

Jean M. Self-Trail*
U.S. Geological Survey, 12201 Sunrise Valley Dr., MS 926A, Reston, VA 20192, USA; *jstrail@usgs.gov

Ellen L. Seefelt
U.S. Geological Survey, 12201 Sunrise Valley Dr., MS 926A, Reston, VA 20192, USA

Claire L. Shepherd
GNS Science, Lower Hutt, New Zealand

Victoria A. Martin
Northern Virginia Community College, Annandale, VA USA

Manuscript submitted 27th September, 2016; revised manuscript accepted 26th June, 2017

Abstract Biostratigraphic and morphometric analyses of calcareous nannofossil assemblages from one outcrop and two cored sections of lower Eocene sediments reveal the presence of two new species: *Tribrachiatus lunatus* sp. nov., and *Tribrachiatus absidatus* sp. nov. Differences between these new species and *Tribrachiatus orthostylus* are discussed. The first occurrence of the two new species is just below the calcareous nannofossil Zone NP11/NP12 boundary, close to the Chron 24r/23n boundary, and thus they are globally useful biostratigraphic markers.

Keywords Calcareous nannofossils, biostratigraphy, early Eocene, taxonomy, *Tribrachiatus*

1. Introduction

From a recent study of lower Eocene sediments from the Atlantic Coastal Plain of Maryland (Self-Trail, 2011), two new calcareous nannofossil species belonging to the genus *Tribrachiatus* are identified. The history of the taxonomy of the genus *Tribrachiatus* is somewhat convoluted and often hard to follow. *Tribrachiatus orthostylus,* the type species of the genus*,* was originally named *Discoaster tribrachiatus* by Bramlette & Riedel (1954), who described a large, triradiate discoaster with or without bifurcations and having slightly bent rays. This species was later used to establish the genus *Tribrachiatus* by Shamrai (1963). Members of this genus were short-lived, first appearing in the early Eocene (Zone NP10) near the top of Chron 24r (Wei & Zhong, 1996) and having their biostratigraphic last occurrence (LO) within Zone NP12, also in the early Eocene. *Tribrachiatus* is thought to have evolved from *Rhomboaster* by rotation and flattening of the nannolith, a process clearly illustrated by Wei & Zhong (1996; their fig. 3). Early forms of *T. orthostylus* (Type A of Wei & Zhong, 1996) are bifurcated (Pl. 3, figs 1, 4–6) and later forms are not.

Although Bramlette & Riedel (1954) stated in their original description that many of these forms have slightly bent rays, this feature is rarely documented, and most published light microscope images of *T. orthostylus* show flat arms (e.g. Wei & Zhong, 1996; Bybell & Self-Trail, 1997; Bown, 2005). However, Bramlette & Sullivan (1961) published one light micrograph (LM) image of a strongly curved specimen, Perch-Nielsen (1977) published one scanning electron micrograph image of a strongly curved *T. orthostylus* from the South Atlantic, and Shepherd & Kulhanek (2016) documented the presence of two forms from New Zealand (Morphotypes A and B) that show curving of two of the three arms.

This paper documents the taxonomy and biostratigraphic ranges of two new species of *Tribrachiatus* in sediments from the United States Atlantic Coastal Plain and New Zealand. The first occurrence (FO) of these new forms is a biostratigraphically useful event in lower Eocene marine sediments. Documentation of the absence of bifurcations in early forms of *T. orthostylus* confirms the report of Wei & Zhong (1996), and the extreme curving of the arms in the two new species described in this paper, *T. lunatus* sp. nov. and *T. absidatus* sp. nov.*,* suggests that the early trend of slightly curving arms in *T. orthostylus* continued and became more pronounced in the late early Eocene.

2. Materials and methods

Specimens of *Tribrachiatus* analyzed and measured in this study were taken from the Bass River (BR) core, located in the Atlantic Coastal Plain of New Jersey (39.6116°N, 74.4366°W), the South Dover Bridge (SDB) core, located in the mid-Atlantic Coastal Plain of Maryland (38.7469°N, 76.0069°W), and from the mid-Waipara River (MW) section located on the Pacific coast of the South Island of New Zealand (43.0539°S, 172.6103°E) (Figure 1).

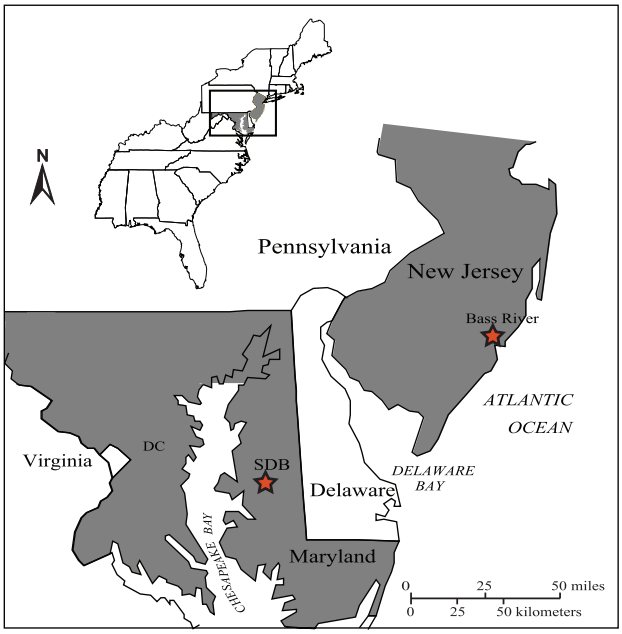

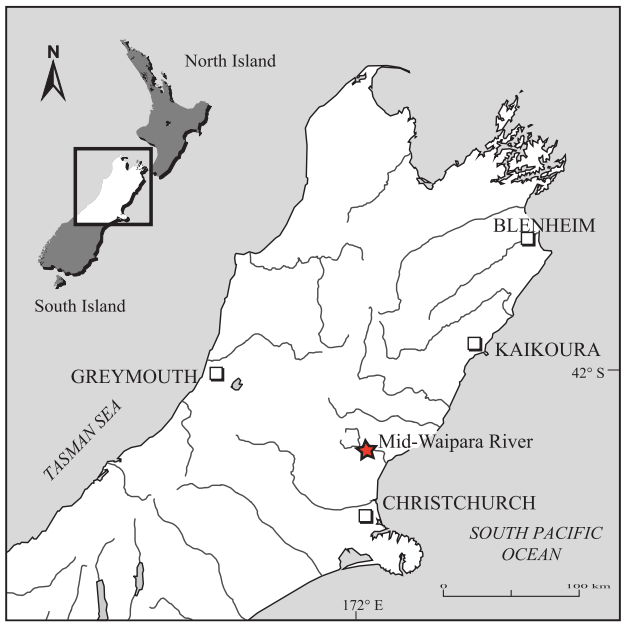

Figure 1: Map showing the location of the South Dover Bridge (SDB) and Bass River (BR) cores (U.S. Atlantic Coastal Plain) and the mid-Waipara River (MW) section, South Island of New Zealand

In the SDB and BR sections, 105 and 133 samples were taken from the Nanjemoy and Manasquan Formations of early Eocene age, respectively. Samples were extracted from the center of freshly broken core segments in order to avoid residual drilling mud contamination. Outcrop material from the MW section is comprised of 30 samples collected in 2012 from an ~11m succession of lower Eocene Ashley Mudstone and six samples collected in 2007 from the basal Ashley Mudstone. The two sample sets were correlated using foraminifera, dinocyst and nannofossil bioevents to produce a composite section. Smear slides were prepared based on the techniques of Bown & Young (1998) and the double slurry method of Watkins & Bergen (2003) and were mounted using Norland Optical Adhesive 61. Slides examined at the U.S. Geological Survey were scanned using a Zeiss Axioplan 2 light microscope at 1250x magnification under cross-polarized (XPL), plane-polarized (PPL) and phase-contrast (PC) light. Slides examined at GNS Science in New Zealand were scanned using an Olympus BX53 microscope at 1000x magnification under XPL, PC and plane-transmitted (PL) light. Scanning electron micrographs were taken at the U.S. Geological Survey using a Hitachi SU-5000 Field Emission scanning electron microscope (SEM). Absolute abundance counts were obtained by counting the number of *Tribrachiatus* specimens per 450 specimens of calcareous nannofossils. To ensure that the biostratigraphic ranges of the new *Tribrachiatus* specimens were accurate, one complete traverse of the short axis of each coverslip was scanned in addition to the 450 specimens and any specimens noted were added to the tally.

The computer program ImageJ, a free program designed and distributed by the National Institute of Health, was used to measure *T. absidatus* and *T. lunatus*. These measurements include 1) the angle formed at the bend in the arm, as measured from a line drawn from the center of the specimen to the tip of the arm, herein designated as the arm angle (see arrow in Figure 2A, 2B); 2) the width between the tips of the two major arms (Figure 2A, 2B); and 3) the outer circumference of a circle transcribed around all three arms. In *T. orthostylus,* only the outer circumference was measured (Figure 2C). These measurements were used to help determine the variation in size and shape for each species and to determine exactly how the two new species differ from each other and *T. orthostylus.*

3. Abundance and biostratigraphic range

Tribrachiatus orthostylus has a distinctly different range than *T. lunatus* and *T. absidatus* (Figure 3). Globally, the FO of *T. orthostylus* occurs near the top of Zone NP10, where it is often used as a proxy for the Zone NP10/NP11 boundary (Martini, 1971; Agnini *et al*., 2014); however, this boundary is truncated in all three studied sections. The top of Zone NP10 is missing from the SDB core (Self-Trail, 2011; Self-Trail *et al*., 2012), as evidenced by the absence of *T. contortus* and the presence of a change in lithology. Miller *et al*. (1998) recorded an unconformable surface at the Zone NP10d/NP11 boundary in the Bass River core based on the presence of rip-up clasts and a change in lithology. A more extensive unconformity is documented from mid-Waipara, where upper Zone NP10 and lowermost Zone NP11 are missing (Shepherd & Kulhanek, 2016). This is clearly seen in Figure 3, where all three species have concurrent first occurrences at MW but not at SDB or BR.

The first rare appearance of *T. absidatus,* which occurs just slightly before the FO of *T. lunatus* in both SDB and

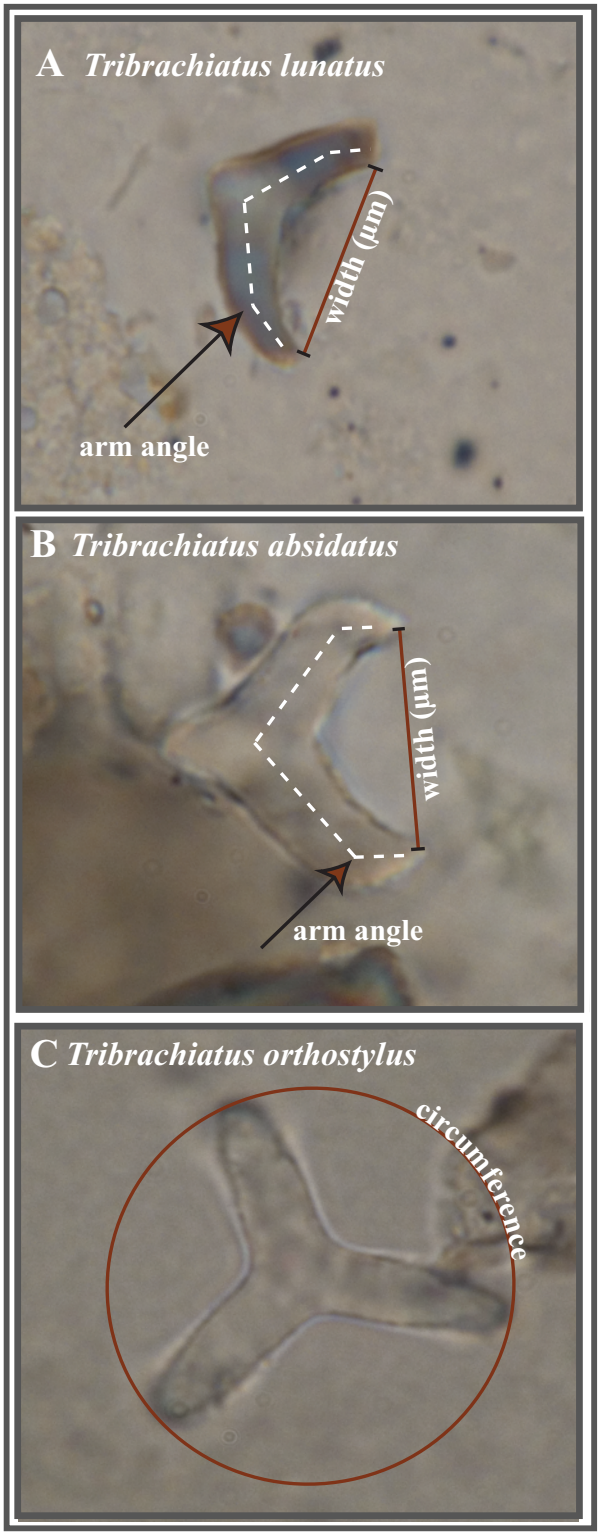

Figure 2: Diagram showing measurement parameters: A) the arm angle and tip-to-tip width of *T. lunatus*, B) the arm angle and tip-to-tip width of *T. absidatus*, and C) the circumference of *T. orthostylus*

BR (Figure 3), is easily missed during routine scanning. A single occurrence of *T. absidatus* in SDB below its FO is due to mixing of sediments at a burrowed contact. Both *T. lunatus* and *T. absidatus* first occur just below the NP11/NP12 boundary, close to the C24r/C23n boundary (Shepherd & Kulhanek, 2016), and therefore these species are useful biostratigraphic markers. The LO of all three forms is simultaneous at all sites and approximates the Zone NP12/NP13 boundary, as defined by Perch-Nielsen (1985). Although a minor unconformity is recorded at this boundary in BR (Miller *et al*., 1998), it appears to be continuous at both SDB and MW (Self-Trail, 2011; Shepherd & Kulhanek, 2016).

4. Morphometric analyses

Morphometric comparison between *T. absidatus* and *T. lunatus* confirms that the two are distinctly different species, despite having nearly identical ranges. Comparison between the circumferences of all three species provides information on changing size through time.

4.1 Arm angle (*T. absidatus* and *T. lunatus*)

The difference in arm angles between *T. absidatus* and *T. lunatus* is clearly delineated in Figure 4. The arm angle in *T. absidatus* is somewhat variable, ranging between 95–141°. Specimens are rarely as perfect as the figured holotype (Pl. 1, fig. 1), often having broken arm tips (Pl. 1, fig. 4) or showing differing asymmetrical angles from arm to arm (Pl. 1, fig. 8). The arm angle in *T. absidatus* at Bass River is slightly bigger than in the other sections, with no recorded specimens below 110°. The arm angle in *T. lunatus* is constrained between 135–160°, with only one outlier in MW having an angle >160° (Figure 4). No significant variation exists between populations from the three cores or through time.

4.2 Tip-to-Tip width (*T. absidatus* and *T. lunatus*)

For *T. absidatus*, the tip-to-tip width of the arms ranges between 6.33–22.4μm, with the majority at MW and SDB falling at or below 10μm (Figure 5). However, the clustering of specimens from Bass River to the right of the 10μm line clearly shows that the specimens from BR are, on average, slightly bigger than those from SDB and MW. The range in the tip-to-tip width between arms in *T. lunatus* is similar to the range for *T. absidatus*, from 6.9–15.6μm, with the majority falling between 8–12μm (Figure 5). It is interesting to note that specimens from MW are smaller than those analyzed from the U.S. Atlantic Coastal Plain. They range between 6.9–10.2μm, with only two outliers of 11.7μm.

4.3 Circumference

The circumference of *T. orthostylus* was measured by drawing a perfect circle around the outside of each specimen, making sure that the circle touched all three arms (Figure 2C). The circumference of specimens from SDB (except for two outliers) and MW is below 250μm, and averaged 143μm and 110μm, respectively (see Figure 6).

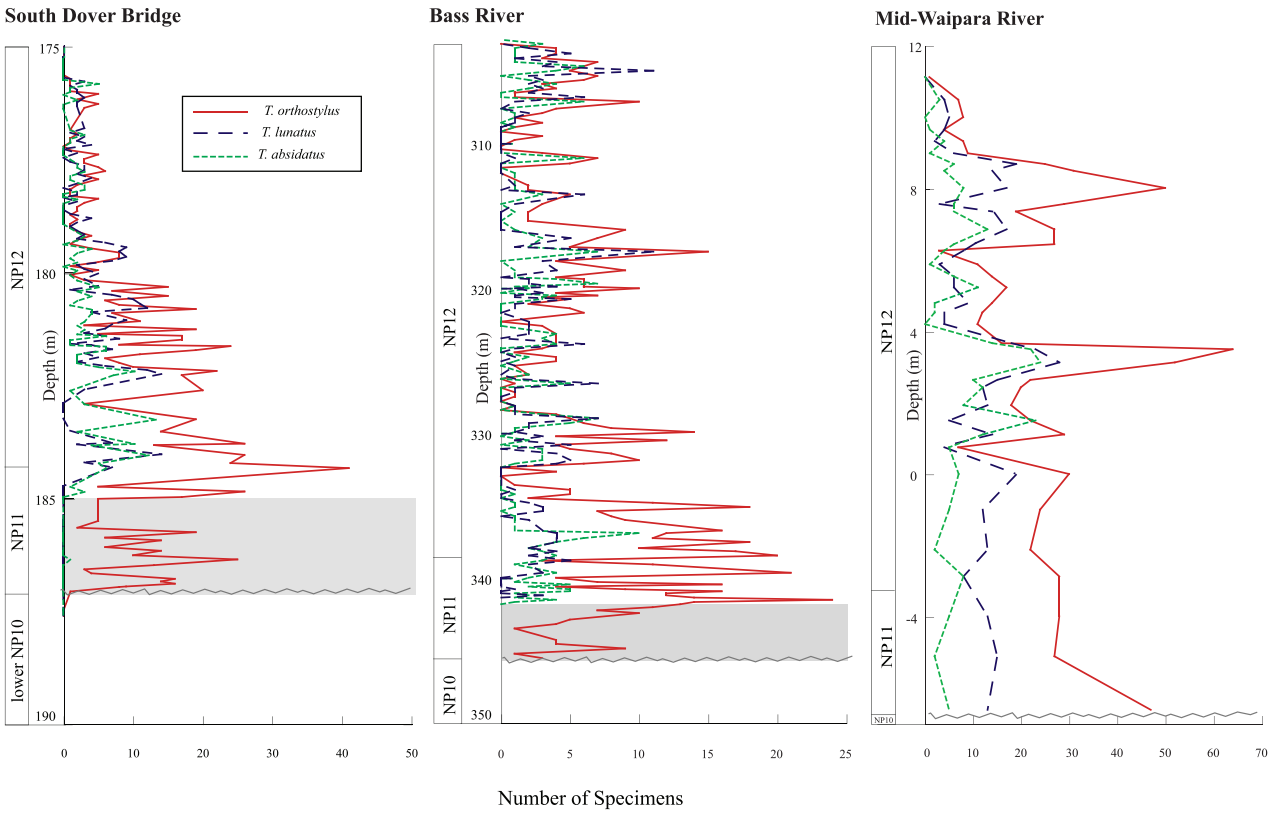

Figure 3: Graphs showing the relative abundance and biostratigraphic range of *T. orthostylus* (red line), *T. absidatus* (green dashed line), and *T. lunatus* (blue dashed line). Shaded area is lowermost Zone NP11, which is missing at the mid-Waipara River section

However, specimens from the basal section of BR (Zone NP11) are significantly bigger and have an average circumference of 287μm and an overall average size of 188μm. Bifurcated specimens from all three sites are typically in the larger size fraction.

For comparison purposes, the circumferences of *T. absidatus* and *T. lunatus* were measured by drawing a circle that followed the outer edge of the two main arms. In BR and SDB, *T. absidatus* averages 143μm and 130μm respectively, and *T. lunatus* averages 132μm and 141μm, respectively. However, specimens from MW are considerably smaller, averaging just 97μm for *T. absidatus* and 89μm for *T. lunatus* (Figure 6).

5. Evolution and discussion

Wei & Zhong (1996) clearly documented the evolution of the genus *Rhomboaster* to *Tribrachiatus* by the rotation and flattening of rhombic cubes through time to three armed forms with bifurcated tips, and a tendency of the arms to curve slightly downward (illustrated here in Pl. 3, fig. 13; Pl. 4, figs 1–3). The continued curvature of two arms in the same plane produced a crescent shape in *T. lunatus* and a vaulted shape in *T. absidatus*, while curvature out of the flat plane and simultaneous reduction of the length of the third arm continued in both species. This trend is recorded by both species in different ways: rounding of the whole body to a crescent shape in *T. lunatus* and bending of the arm tips by >95° in *T. absidatus*. Although the angle between arms of *T. orthostylus* must increase during the transition to *T. absidatus* and *T. lunatus*, preliminary measurements of specimens from BR did not show any change. However, upper Zone NP10 sections are often very thin or lacking on the Atlantic Coastal Plain (Gibson & Bybell, 1994; Self-Trail, 2011) and it is probable that this section was not sampled or is missing in BR.

The slightly longer third arm and sharply defined interior angle of *T. absidatus*, coupled with its slightly earlier appearance in SDB and BR (see Figure 3), suggests that *T. absidatus* evolved from *T. orthostylus* first, quickly followed by the evolution of *T. lunatus*. Although *T. lunatus* and *T. absidatus* have very similar ranges, Figure 4 illustrates the two are distinct species, as *T. absidatus* has a consistently smaller average arm angle (<140°) than *T. lunatus* (>140°).

It is interesting to note that specimens of *T. lunatus*, *T. absidatus* and *T. orthostylus* in the MW section are consistently smaller than at BR and SDB (Figures 5, 6). This suggests either an intrinsic size difference between the Atlantic and Pacific populations or a contributing paleoceanographic factor in the local formation of the coccoliths. Sediments from the MW section were deposited at upper bathyal depths (Morgans *et al*., 2005; Hollis *et al*., 2012), while sediments from SDB and BR were deposited

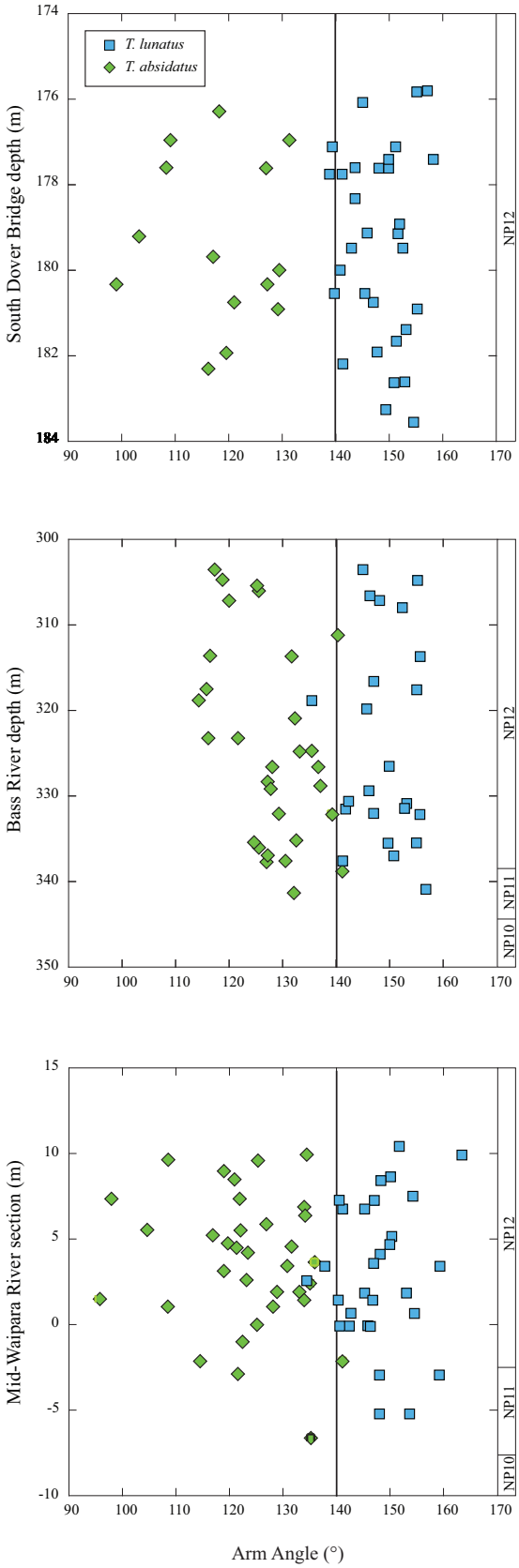

Figure 4: Comparison between the arm angles of *T. absidatus* (green diamonds) and *T. lunatus* (blue squares). Note the clear separation of angles between the two species. Solid vertical black line denotes the 140° arm angle

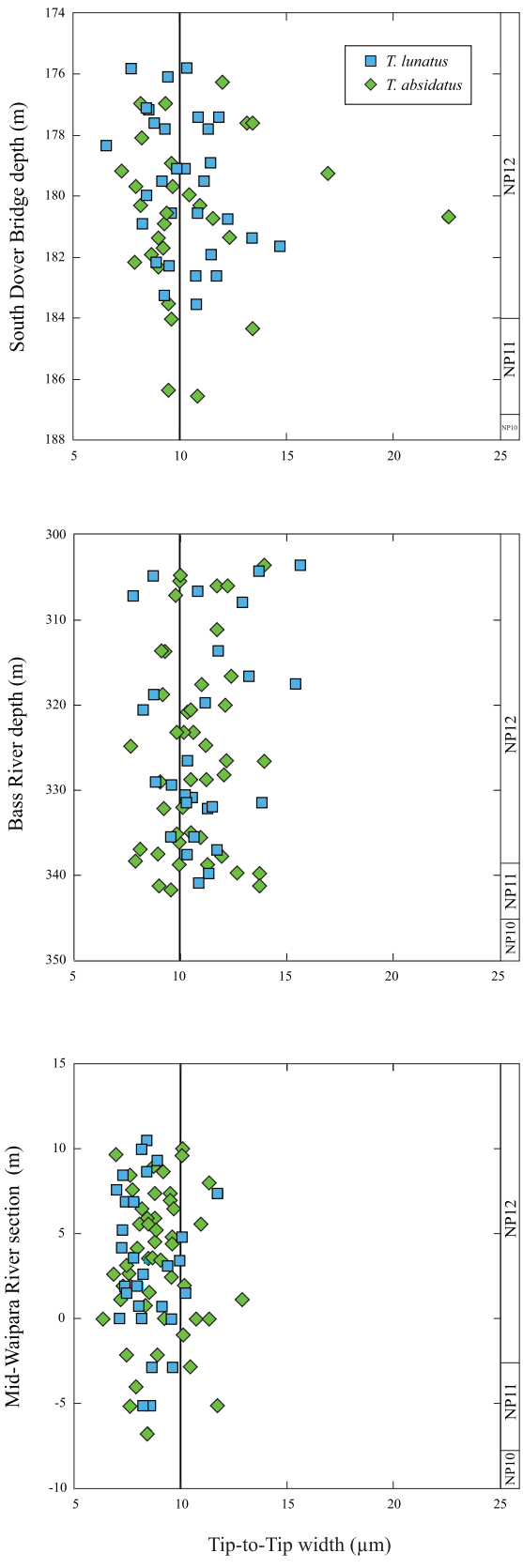

Figure 5: Comparison between the tip-to-tip width of *T. absidatus* (green diamonds) and *T. lunatus* (blue squares). Note that the width of specimens from the mid-Waipara River section is smaller than those from South Dover Bridge and Bass River. The solid black vertical line denotes a width of 10μm

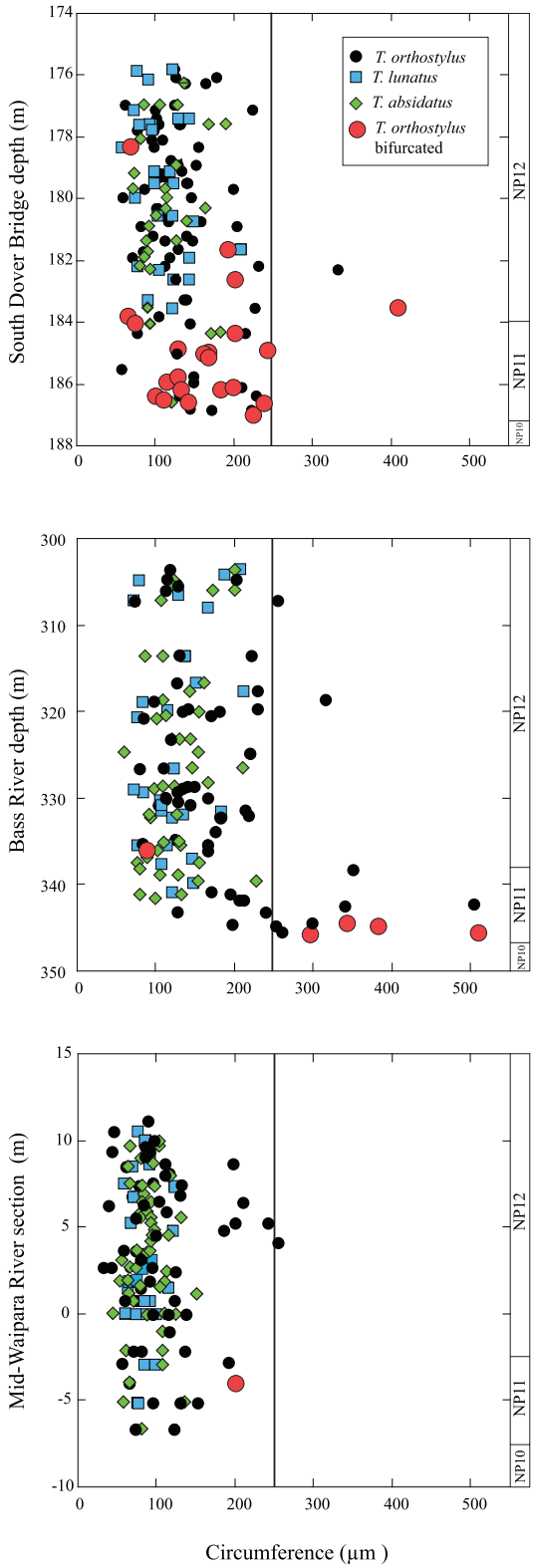

Figure 6: Comparison between the circumference of *T. absidatus* (green diamonds), *T. lunatus* (blue squares) and *T. orthostylus* (black circles) in South Dover Bridge, Bass River and mid-Waipara River. Large red circles show specimens with bifurcations. Note that these occur in the deepest part of the section at each site, with one exception at SDB. The relative paucity of bifurcated specimens at mid-Waipara River is due to an unconformity at the base of NP11

in mid- to outer-shelf environments, respectively, and were relatively proximal to shore (Kopp *et al*., 2009; Self-Trail *et al*., 2012). Thus, factors relating to salinity, water clarity and oxygenation could have imposed restrictions on productivity and size.

Changing conditions through time also resulted in a corresponding change in size and shape. For example, the oldest specimens of *T. orthostylus* in BR are considerably bigger than the correlative specimens in SDB, but by Zone NP12 time (~53Ma) the two populations are similar in size (Figure 6). The absence of lower Zone NP11 sediments from MW makes size comparisons to the other two sites impossible. Additionally, bifurcated *T. orthostylus* are common at the beginning of this species range, but disappear by mid-NP12 time.

6. Systematic Paleontology

All figured specimens and type species are stored in the calcareous nannofossil laboratory at the U.S. Geological Survey in Reston, Virginia, USA. All light micrograph specimens were taken at the same magnification (x2000). Scanning electron micrograph image scale bars are 5μm unless otherwise noted. Nannolith shape terminology follows the guidelines of Young *et al*. (1997).

Family **RHOMBOASTERACEAE** Bown, 2005

Tribrachiatus absidatus sp. nov.
Pl. 1, figs 1–14
2016 *Tribrachiatus* Morphotype B, Shepherd & Kulhanek, Pl. 11, figs 21–22

Derivation of name: From the Latin for "vaulted", a reference to its resemblance to the vaulted interior of a classical building such as a cathedral.

Description: A medium to large, triradiate nannolith having two straight to slightly curved arms of equal length that exhibit a 95–140° bend near their pointed tips, and a smaller third arm that is less than half the length of the two main arms. The interior angle is between 110–140°. Width between ray tips is typically <15μm (Figure 5). Specimens from all three locations are commonly overgrown and exhibit high-order birefringence colors.

Differentiation: *Tribrachiatus absidatus* exhibits a broad range of morphological variation, and overgrowth can make it difficult to distinguish it from broken specimens of *T. orthostylus* and *T. lunatus*. *Tribrachiatus absidatus* can be differentiated from *T. lunatus* by the presence of a vaulted interior angle rather than a crescent arc and by the presence of bent tips at the end of the two main arms. Arm tips are prone to breaking off (Pl. 1, fig. 4). Typically, the third arm of *T. absidatus* is slightly longer than the third arm of *T. lunatus* (e.g. Pl. 1, fig. 9).

Dimensions: The tip-to-tip width between the two main arms of *T. absidatus* ranges from 6.33–22.49μm and the interior angle ranges between 94–151° (n=126).

Holotype: Pl. 1, fig. 1

Paratype: Pl. 1, fig. 2

Type locality: South Dover Bridge core, Maryland, USA

Type level: lower Eocene, Sample N13869, 180.35m (Zone NP12)

Occurrence: Zones NP 11–12

Tribrachiatus lunatus sp. nov.
Pl. 2, figs 1–14; Pl. 4, figs 10, 14–15

1961 *Discoaster tribrachiatus* Bramlette & Sullivan, Pl. 13, fig. 11
1977 *Tribrachiatus orthostylus* Perch-Nielsen, Pl. 14, fig. 7
2016 *Tribrachiatus* morphotype A, Shepherd & Kulhanek, Pl. 11, fig. 20

Derivation of name: From the Latin for crescent shaped, a reference to its resemblance to a crescent moon.

Description: Medium to large, triradiate nannolith with two curved arms of equal length and a third arm that forms a small nub, occasionally curved, that lies midway between the two other arms. Ray tips of the two main arms typically taper to a sharp point and width between ray tips is <15μm (Figure 5). When oriented so that the small third arm is facing upward towards the lens, it has bright birefringence colors (often green or pink), and the specimen looks like a marquise diamond ring (Pl. 2, fig. 13). The crescent shape in larger specimens is somewhat flattened when compared to smaller specimens, which are more rounded. Specimens from all sections are commonly overgrown and exhibit high-order birefringence colors (Pl. 2, fig. 13).

Differentiation: *Tribrachiatus lunatus* differs from *T. absidatus* by having a rounded interior that is crescent shaped and a smaller third arm. Additionally, *T. lunatus* lacks the bent arm tips that are present in *T. absidatus*. It can sometimes be difficult to distinguish between overgrown specimens of *T. lunatus* and *T. absidatus* using XPL (e.g., compare specimens of *T. lunatus* [Pl. 2, fig. 10-a] with Pl. 1, fig. 11-a), but is easier using PC (compare Pl. 2, fig. 10-b to Pl. 1, fig. 11-b). Although curved specimens of *T. orthostylus* can sometimes be mistaken for *T. lunatus* if viewed from an odd angle, *T. orthostylus* typically has a much lower order birefringence color than does *T. lunatus* and is usually gray in color.

Dimensions: The tip-to-tip width between the two main arms of *T. lunatus* has a range of 6.9–15.6μm (n=92).

Holotype: Pl. 2, fig. 1

Paratype: Pl. 2, fig. 4

Type locality: mid-Waipara River section, Canterbury Basin, New Zealand

Type level: lower Eocene, Sample F41309, 7.36m (Zone NP12)

Occurrence: Zones NP 11–12

Tribrachiatus orthostylus Shamrai, 1963
Pl. 3, figs 1–15; Pl. 4, figs 1–9, 11–13

Remarks: *Tribrachiatus orthostylus* is a triradiate form showing low order birefringence colors and having bifurcations at the tips of the arms in older specimens (Pl. 3, figs 1, 3–6). The circumference has a range of 42–508μm; larger specimens are recorded from BR (Figure 6).

Occurrence: upper Zone NP10-NP12

Acknowledgements

We thank Jim Browning, Rutgers Core Repository, for access to the Bass River core, and Brett Valentine (USGS) for valuable assistance with the SEM. Ric Jordan (Yamagata University) provided invaluable technical advice on systematics. An early draft of the manuscript benefitted from the reviews of Laurel Bybell and Marci Robinson (both of USGS). The authors wish to thank David Bord (ALS) and Richard Howe (Chevron) for their thoughtful reviews. Funding for this paper was provided in part by the National Cooperative Geologic Mapping and the Climate and Land Use Change Programs (USGS), and by the New Zealand Government through the Marsden Fund. Any use of trade, firm, or product names is for descriptive purposes only and does not imply endorsement by the U.S. Government.

References

Agnini, C., Fornaciari, E., Raffi, I., Catanzariti, R., Palike, H., Backman, J. & Rio, D. 2014. Biozonation and biochronology of Paleogene calcareous nannofossils from low and middle latitudes. *Newslettters on Stratigraphy*, **47**(2): 131–181.

Bown, P.R. 2005. Palaeogene calcareous nannofossils from the Kilwa and Lindi areas of coastal Tanzania (Tanzania Drilling Project 2003–4). *Journal of Nannoplankton Research*, **27**(1): 21–96.

Bown, P.R. & Young, J.R. 1998. Techniques. *In*: P.R. Bown (Ed.). *Calcareous Nannofossil Biostratigraphy*. Kluwer Academic Press: 16–28.

Bramlette, M.N. & Riedel, W.R. 1954. Stratigraphic value of Discoasters and some other microfossils related to recent Coccolithophores. *Journal of Paleontology*, **28**(4): 385–403.

Bramlette, M.N. & Sullivan, F.R. 1961. Coccolithophorids and related Nannoplankton of the early Tertiary in California. *Micropaleontology*, **7**(2): 129–188.

Bybell, L.M. & Self-Trail, J.M. 1997. Late Paleocene and early Eocene calcareous nannofossils from three boreholes in an onshore-offshore transect from New Jersey to the Atlantic Continental rise. *Proceedings of the ODP, Scientific Results,* **150X**: 91–110.

Gibson, T.G. & Bybell, L.M. 1994. Paleogene stratigraphy of the Solomons Island, Maryland corehole. *U.S. Geological Survey Open-file Report,* **94–708**: 39pp.

Hollis, C.J., Taylor, K.W.R., Handley, L., Pancost, R.D., Huber, M., Creech, J.B., *et al*. 2012. Early Paleogene temperature history of the Southwest Pacific Ocean: Reconciling proxies and models. *Earth and Planetary Science Letters,* **349–350**: 53–66. doi: 10.1016/j.epsl.2012.06.024.

Kopp, R.E., Schumann, D., Raub, T.D., Powars, D.S., Godfrey, L.V., Swanson-Hysell, N.L., Maloof, A.C. & Vali, H. 2009. An Appalachian Amazon? Magnetofossil evidence for the development of a tropic river-like system in the mid-Atlantic United States during the Paleocene-Eocene thermal maximum. *Paleoceanography*, **24**: PA4211, doi: 10.1029/2009PA001783.

Martini, E. 1971. Standard Tertiary and Quaternary calcareous nannoplankton zonation, *In*: A. Farinacci (Ed.). *Proceedings of the Second Planktonic Conference*, Roma, 1970, *Edizioni Tecnoscienza*, Rome, **2**: 739–785.

Miller, K.G., Sugarman, P.J., Browning, J.V., *et al*., 1998. Bass River Site. *Proceedings of the ODP, Initial Reports*, **174AX**: 1–39.

Morgans, H.E.G., Jones, C.M., Crouch, E.M., Field, B.D., Raine, J.I., Strong, C.P., *et al*. 2005. Upper Cretaceous to Eocene stratigraphy and sample collections, mid-Waipara River section, North Canterbury. *Institute of Geological & Nuclear Sciences report 2003/08.*

Perch-Nielsen, K. 1977. Albian to Pleistocene calcareous nannofossils from the western South Atlantic, DSDP Leg 39. *Proceedings of the ODP, Initial Reports*, **39**: 699–823.

Perch-Nielsen, K. 1985. Cenozoic calcareous nannofossils. *In*: H. Bolli, K. Perch-Nielsen & J.B. Saunders (Eds). *Plankton Stratigraphy*. Cambridge University Press, Cambridge: 427–554.

Self-Trail, J.M. 2011. Paleogene calcareous nannofossils of Southern Maryland, South Dover Bridge core, USA. *Journal of Nannoplankton Research,* **32**: 1–28.

Self-Trail, J.M., Powars, D.S., Watkins, D.K. & Wandless, G.A. 2012. Calcareous nannofossil assemblage changes across the Paleocene-Eocene Thermal Maximum: Evidence from a shelf setting. *Marine Micropaleontology*, **92–93**: 61–80.

Shamrai, I.A. 1963. Certain forms of Upper Cretaceous and Paleogene coccoliths and discoasters from the southern Russian Platform, *Izvestiya Vysshith Uchebnyk Zavedenii Geologiaya i Razvedka*, **6**: 27–40.

Shepherd, C.L. & Kulhanek, D.K. 2016. Eocene nannofossil biostratigraphy of the mid-Waipara River section, Canterbury Basin, New Zealand. *Journal of Nannoplankton Research*, **36**(1): 33–59.

Watkins, D.K., & Bergen, J.A., 2003. Late Albian adaptive radiation in the calcareous nannofossil genus *Eiffellithus*. *Micropaleontology*, **49**(3): 231–251.

Wei, W. & Zhong, S. 1996. Taxonomy and magnetobiochronology of *Tribrachiatus* and *Rhomboaster*, two genera of calcareous nannofossils. *Journal of Paleontology*, **70**(1): 7–22.

Young, J.R., Bergen, J.A., Bown, P.R., Burnett, J.A., Fiorentino, A., Jordan, R.W., Kleijne, A., van Niel, B.E., *et al*. 1997. Guidelines for coccolith and calcareous nannofossil terminology. *Palaeontology*, **40**(4): 875–912.

Plate 1. *Tribrachiatus absidatus*

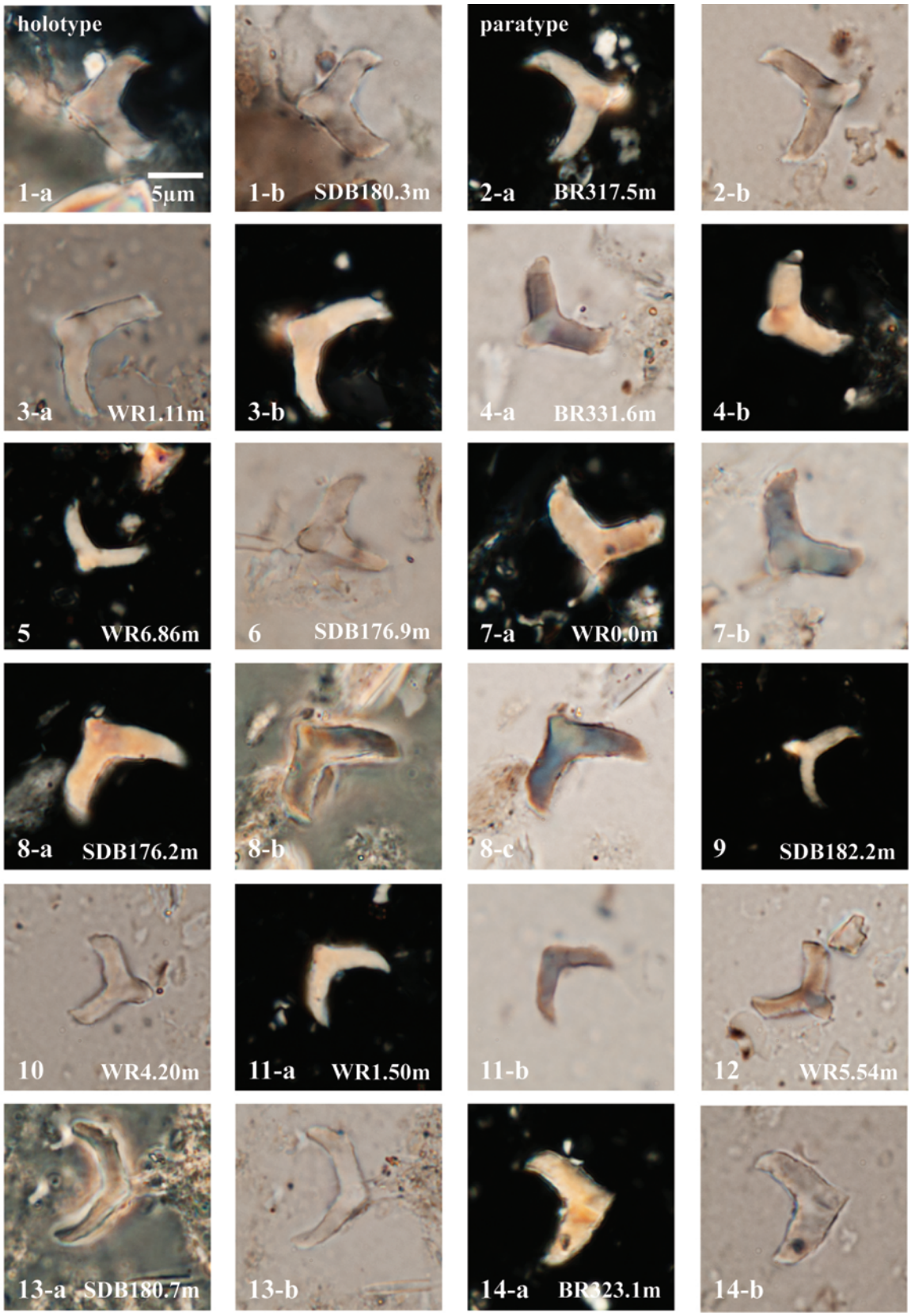

Illustrated specimens in XPL, PPL, and PC. Specimens are identified by section and depth. BR = Bass River; SDB = South Dover Bridge; WR = mid-Waipara River

Plate 2. *Tribrachiatus lunatus*

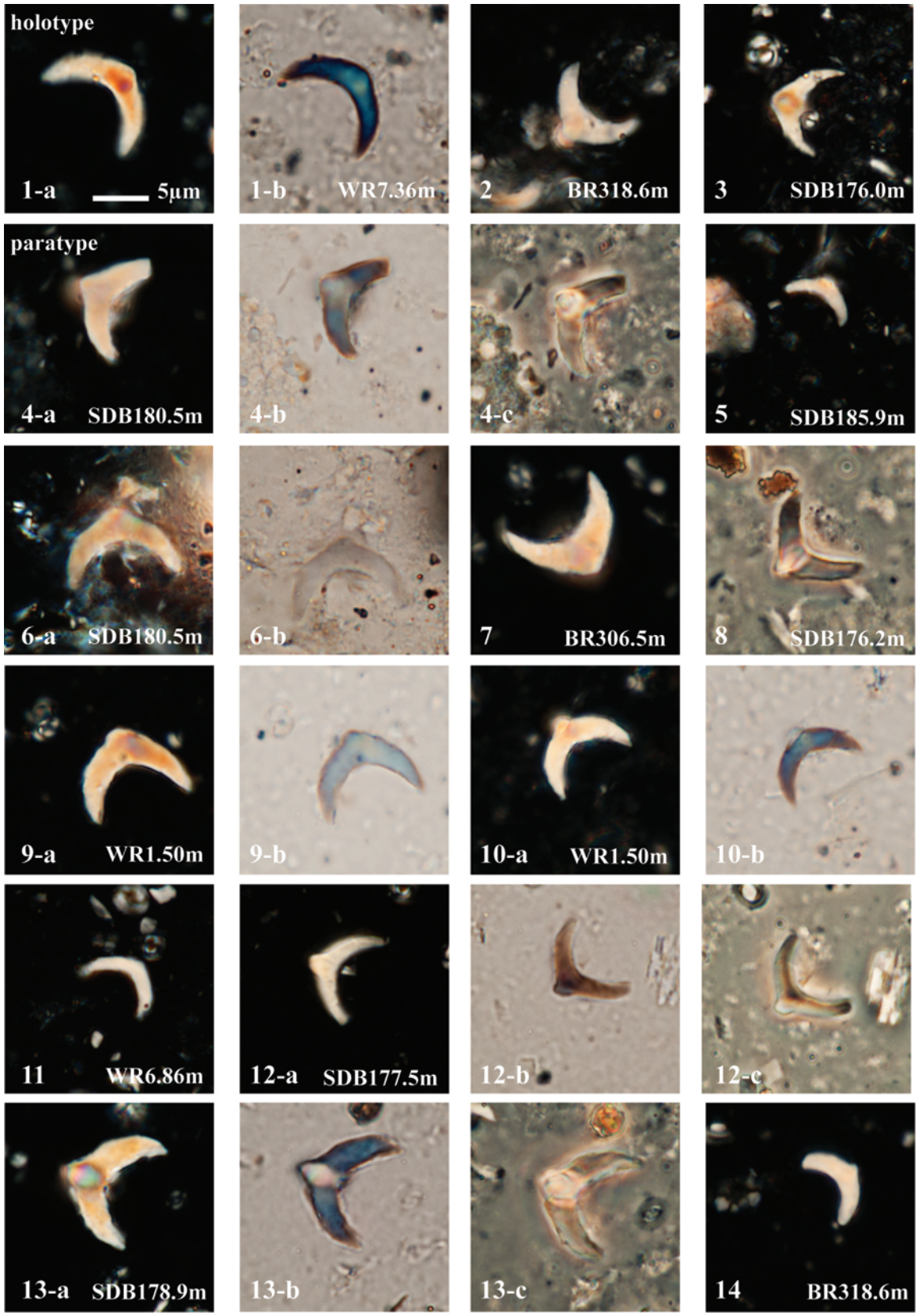

Illustrated specimens in XPL, PPL, and PC. Specimens are identified by section and depth. BR = Bass River; SDB = South Dover Bridge; WR = mid-Waipara River

Plate 3. *Tribrachiatus orthostylus*

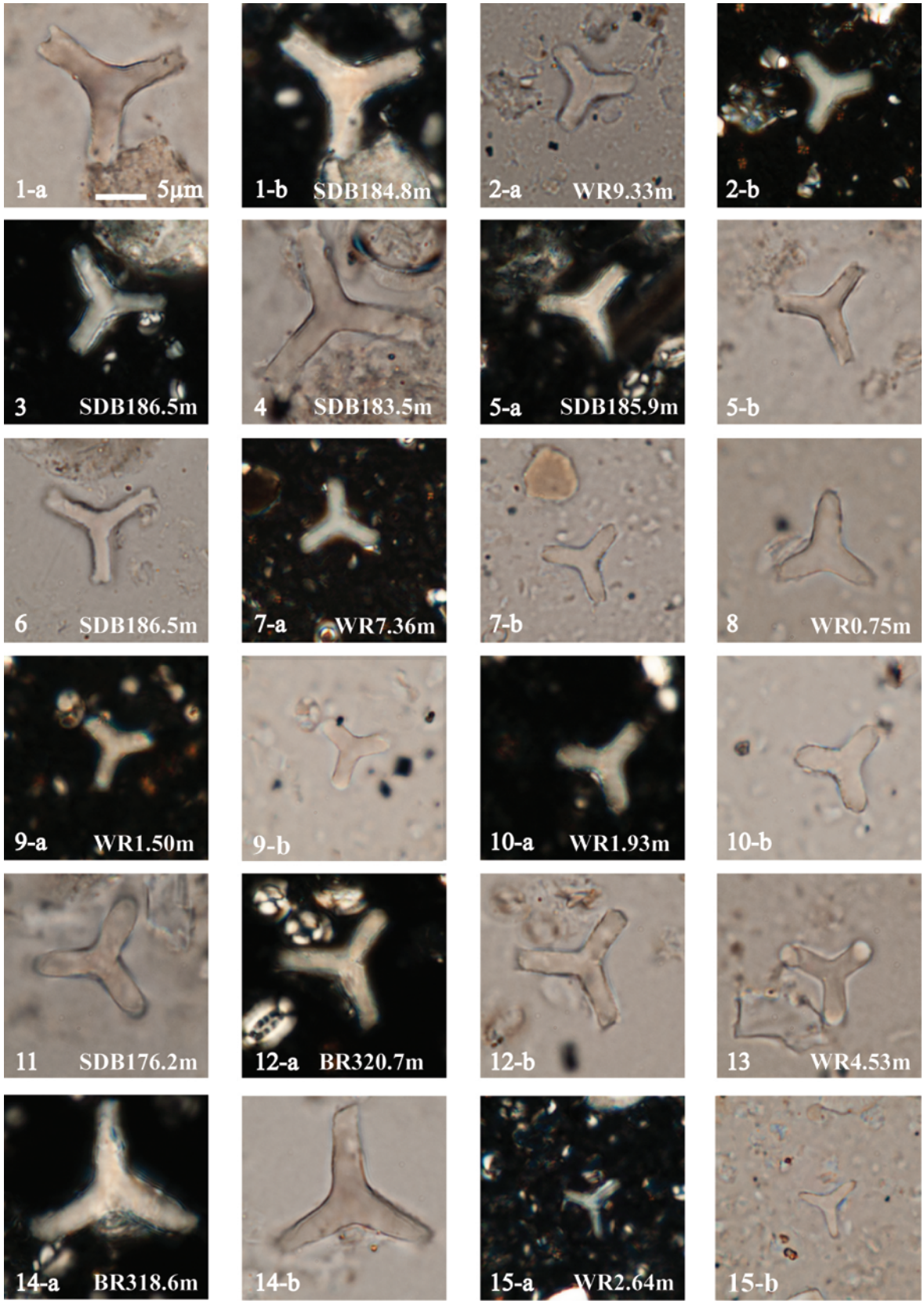

Illustrated specimens in XPL, PPL, and PC. Specimens are identified by section and depth. BR = Bass River; SDB = South Dover Bridge; WR = mid-Waipara River

Plate 4. SEM images

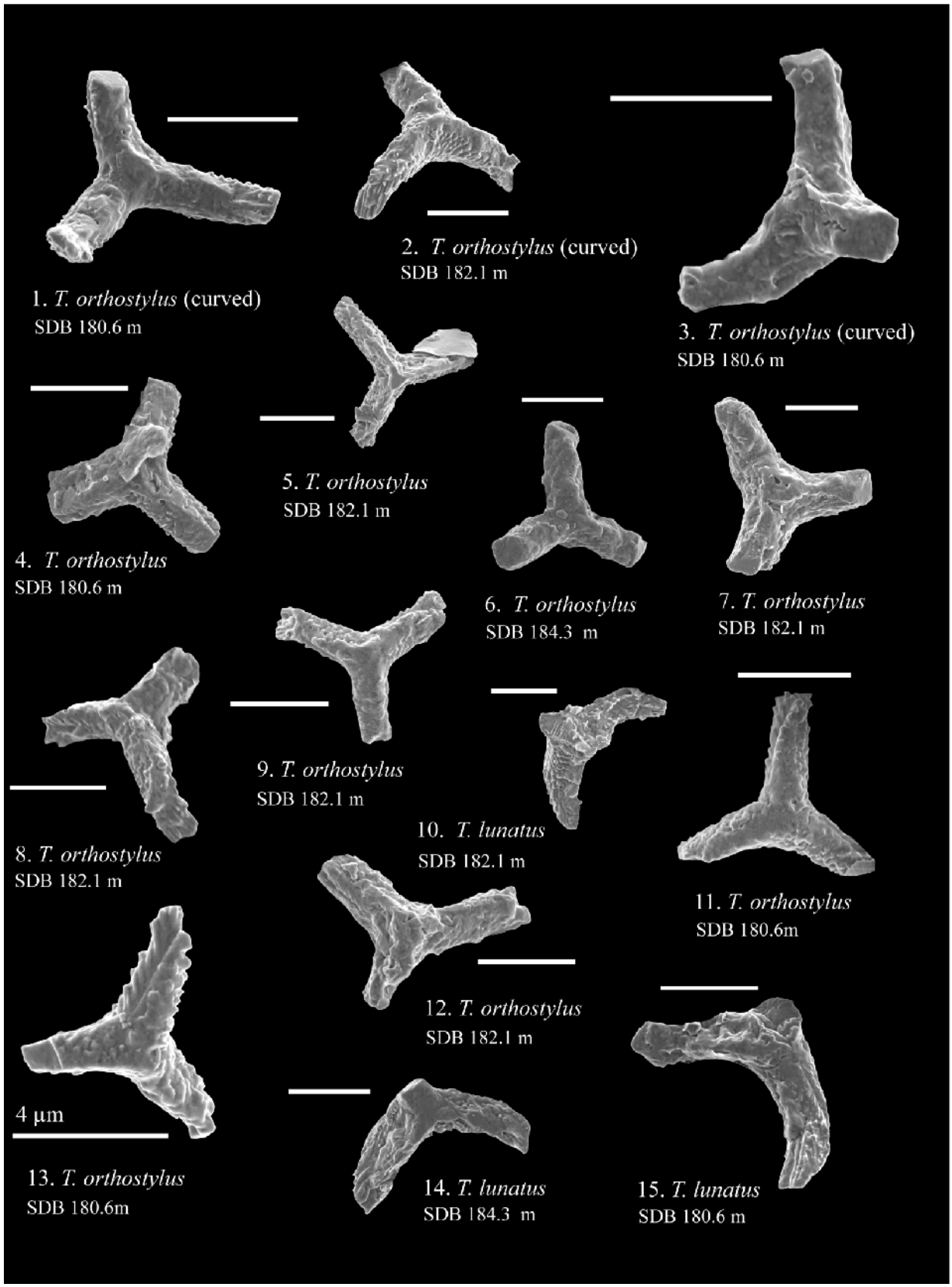

Tribrachiatus lunatus and *T. orthostylus*. Specimens are identified by section and depth. SDB = South Dover Bridge. SEM image scale bars are 5μm unless otherwise noted